

Mass spectra of Z_c and Z_b exotic states as hadron molecules

Wei Chen and T. G. Steele

*Department of Physics and Engineering Physics,
University of Saskatchewan, Saskatoon, SK, S7N 5E2, Canada*

Hua-Xing Chen*

*School of Physics and Nuclear Energy Engineering and International Research Center
for Nuclei and Particles in the Cosmos, Beihang University, Beijing 100191, China*

Shi-Lin Zhu†

*School of Physics and State Key Laboratory of Nuclear Physics and Technology, Peking University, Beijing 100871, China
Collaborative Innovation Center of Quantum Matter, Beijing 100871, China
Center of High Energy Physics, Peking University, Beijing 100871, China*

We construct charmonium-like and bottomonium-like molecular interpolating currents with quantum numbers $J^{PC} = 1^{+-}$ in a systematic way, including both color singlet-singlet and color octet-octet structures. Using these interpolating currents, we calculate two-point correlation functions and perform QCD sum rule analyses to obtain mass spectra of the charmonium-like and bottomonium-like molecular states. Masses of the charmonium-like $\bar{q}c\bar{c}q$ molecular states for these various currents are extracted in the range 3.85–4.22 GeV, which are in good agreement with observed masses of the Z_c resonances. Our numerical results suggest a possible landscape of hadronic molecule interpretations of the newly-observed Z_c states. Mass spectra of the bottomonium-like $\bar{q}b\bar{b}q$ molecular states are similarly obtained in the range 9.92–10.48 GeV, which support the interpretation of the $Z_b(10610)$ meson as a molecular state within theoretical uncertainties. Possible decay channels of these molecular states are also discussed.

PACS numbers: 12.38.Lg, 11.40.-q, 12.39.Mk

Keywords: exotic state, molecule, QCD sum rules, two-point correlation function

I. INTRODUCTION

To date, there are eight members in the family of the electrically charged states: $Z_c(3900)$, $Z_c(4020)$, $Z_1(4050)$, $Z_2(4250)$, $Z_c(4200)$, $Z(4430)$ and $Z_b(10610)$, $Z_b(10650)$ observed in decays into final states containing a pair of heavy quarks [1–11]. Being not conventional $Q\bar{Q}$ states because of their charge, they must be exotic with minimal quark contents $Q\bar{Q}u\bar{d}$.

The first charged exotic state, $Z(4430)^+$ was observed in the B meson decay process $\bar{B}^0 \rightarrow \psi(2S)\pi^+K^-$ by the Belle Collaboration [1] in 2007. Recently, the LHCb experiment repeated the Belle analysis and confirmed the existence of $Z(4430)^+$ with $J^P = 1^+$ [2]. The broad doubly peaked structure $Z_1(4050)^+$ and $Z_2(4250)^+$ are resonances in the $\pi^+\chi_{c1}$ channel, which were found by the Belle Collaboration [3] in 2008. In 2013, the BESIII Collaboration reported $Z_c(3900)^+$ in the process of $Y(4260) \rightarrow J/\psi\pi^+\pi^-$ [4], which was confirmed later by Belle [5] and CLEO data [6]. The BESIII Collaboration also observed the $Z_c(4020)$ resonance in the $e^+e^- \rightarrow \pi^+\pi^-h_c$ and $e^+e^- \rightarrow (D^*\bar{D}^*)^\pm\pi^\mp$ processes [7, 8]. Very recently, two new charged charmonium-like resonances $Z_c(4200)^+$ [9] and $Z_c(4050)$ [10] were observed by the Belle Collaboration in the processes of $\bar{B}^0 \rightarrow J/\psi\pi^-K^+$ and $e^+e^- \rightarrow \pi^+\pi^-\psi(2S)$, respectively. For the charged bottomonium-like states, $Z_b(10610)$ and $Z_b(10650)$ were reported by the Belle Collaboration in the $\pi^\pm\Upsilon(nS)$ and $h_b\pi^\pm$ mass spectra in the $\Upsilon(5S)$ decay [11]. One can consult Refs. [12–14] for recent reviews of these charged resonances.

These exotic charged resonances are isovector states with quantum numbers $I^G J^P = 1^+ 1^+$ while their neutral partners have charge-conjugation parity $C = -1$. As four-quark states with quark contents $\bar{c}c\bar{u}d/\bar{b}b\bar{u}d$, these newly observed resonances were usually studied as hadron molecules and tetraquark states. These two hadron configurations are totally different. At the hadronic level, the hadron molecules are loosely bound states of two heavy mesons formed by the exchange of long-range color-singlet mesons. Tetraquarks are more compact four-body states which are generally bound by the QCD colored force between diquarks at the quark-gluon level. There are many theoretical studies on

*Electronic address: hxchen@buaa.edu.cn

†Electronic address: zhushl@pku.edu.cn

these charged resonances; see Ref. [14] for a recent review. $Z_c(3900)^+$ was interpreted as a $\bar{D}D^*$ molecular state in Refs. [15–17]. $Z_c(4020)^+$ was speculated to be a $D^*\bar{D}^*$ molecular state in Refs. [18–20]. $Z_c(4200)^+$ is much broader than other charged resonances in this family so that it was studied as a good candidate for a tetraquark state in Refs. [21, 22]. It was also studied as a molecular state in Ref. [23]. $Z(4430)^+$ was described as a tetraquark state in Refs. [24–26] and a $D^*\bar{D}_1$ molecular state in Refs. [27–29]. $Z_b(10610)$ and $Z_b(10650)$ were interpreted as $\bar{B}B^*$ and \bar{B}^*B^* molecular states in Refs. [30, 31].

The mass spectra of the charmonium-like and bottomonium-like tetraquark states were studied comprehensively in Refs. [32–35, 37]. In Ref. [35], the masses of the charmonium-like tetraquark states with $I^G J^{PC} = 1^+ 1^{+-}$ were obtained from various currents in the range 4.0–4.2 GeV, which were consistent with the spectra of the charged Z_c states. However, the molecular interpretations for these states are slightly more natural, especially for the $Z_c(3900)^+$ and $Z_c(4020)^+$ mesons which lie very close to the open-charm thresholds. In this work, we will study the mass spectra of the charmonium-like ($\bar{q}c\bar{c}q$) and bottomonium-like ($\bar{q}b\bar{b}q$) molecular states with the quantum numbers $J^{PC} = 1^{+-}$ using the approach of QCD sum rules [38–40], which is used to study the hadron properties of the lowest bound state. The masses of higher excited states are not easy to be calculate in QCD sum rules because their contributions are exponentially suppressed. However, there have been some attempts to study the orbitally excited nucleon [41–43]. We try to explain the newly observed Z_c and Z_b states as molecular states and compare the difference between the molecular and tetraquark configurations. We note that we shall consider both the color singlet-singlet molecular structure and the color octet-octet “molecular” structure.

There are many investigations of possible molecular states by using hadronic level Feynman diagrams, particularly investigations in the framework of the one boson exchange model [17]. Generally speaking, this kind of study employs an effective Lagrangian to derive either the scattering amplitude or the effective potential. Besides the pion, quite a few other mesons are introduced which lead to many new coupling constants which have not been completely determined experimentally. Moreover, a form factor is always introduced at each vertex in order to suppress the high momentum exchange effect, which requires a new cutoff parameter. In other words, there exists some inherent uncertainties with the approach at the hadronic level. The QCD sum rule approach and the formalism at the hadronic level are complementary to each other.

The paper is organized as follows. In Sect. II, we construct the molecular interpolating currents with $J^{PC} = 1^{+-}$ for the Z_c and Z_b states. In Sect. III, we introduce the QCD sum rule formalism concisely and calculate the two-point correlation functions and spectral densities using these interpolating currents. We perform numerical analyses and extract the mass spectra and coupling constants for the charmonium-like and bottomonium-like molecular states in Sect. IV. In the last section, we summarize our results and discuss the possible decay modes for these molecular states.

II. MOLECULAR INTERPOLATING CURRENTS FOR THE Z_c AND Z_b STATES

There are two different types of four-quark operators: diquark-antidiquark type tetraquark fields and meson-meson type molecule fields. The former kind of operator is composed of a pair of diquark and antidiquark fields ($[qq][\bar{q}\bar{q}]$) while the latter one is composed of a pair of meson (or meson-like) fields ($[q\bar{q}][q\bar{q}]$). The diquark-antidiquark type tetraquark fields have been constructed and studied systematically in Refs. [34, 35, 37]. Particularly, there are eight independent diquark-antidiquark tetraquark fields with $J^{PC} = 1^{+-}$, which have been systematically constructed and studied in Ref. [35]. These eight tetraquark currents can be transformed into the combinations of other eight meson-meson type molecule currents by using Fierz transformations. In this paper, we systematically construct these eight meson-meson type molecule fields, and use them to study the charged Z_c^+ resonances as molecular states.

The color structure of a molecule field ($[q\bar{Q}][Q\bar{q}]$) can be written as

$$\begin{aligned} (\mathbf{3} \otimes \bar{\mathbf{3}})_{[q\bar{Q}]} \otimes (\mathbf{3} \otimes \bar{\mathbf{3}})_{[Q\bar{q}]} &= (\mathbf{1} \oplus \mathbf{8})_{[q\bar{Q}]} \otimes (\mathbf{1} \oplus \mathbf{8})_{[Q\bar{q}]} \\ &= (\mathbf{1} \otimes \mathbf{1}) \oplus (\mathbf{1} \otimes \mathbf{8}) \oplus (\mathbf{8} \otimes \mathbf{1}) \oplus (\mathbf{8} \otimes \mathbf{8}) \\ &= \mathbf{1} \oplus \mathbf{8} \oplus \mathbf{8} \oplus (\mathbf{1} \oplus \mathbf{8} \oplus \mathbf{8} \oplus \mathbf{10} \oplus \bar{\mathbf{10}} \oplus \mathbf{27}) . \end{aligned} \quad (1)$$

The two color singlet structures in Eq. (1) come from the $(\mathbf{1}_{[q\bar{Q}]} \otimes \mathbf{1}_{[Q\bar{q}]})$ and $(\mathbf{8}_{[q\bar{Q}]} \otimes \mathbf{8}_{[Q\bar{q}]})$ terms in the second step, respectively. In other words, the two mesonic fields $[q\bar{Q}]$ and $[Q\bar{q}]$ should have the same color structures to compose a color singlet molecular current.

For $(\mathbf{1}_{[q\bar{Q}]} \otimes \mathbf{1}_{[Q\bar{q}]})$ structure, we can obtain eight independent molecule fields with $J^P = 1^+$ by considering only

S-wave of the angular momentum between the two mesonic fields. Four of them are

$$\begin{aligned} J_{1\mu,L}^{(1)} &= (\bar{q}_a \gamma_5 Q_a)(\bar{Q}_b \gamma_\mu q_b), \\ J_{2\mu,L}^{(1)} &= (\bar{q}_a Q_a)(\bar{Q}_b \gamma_\mu \gamma_5 q_b), \\ J_{3\mu,L}^{(1)} &= (\bar{q}_a \gamma^\alpha Q_a)(\bar{Q}_b \sigma_{\alpha\mu} \gamma_5 q_b), \\ J_{4\mu,L}^{(1)} &= (\bar{q}_a \gamma^\alpha \gamma_5 Q_a)(\bar{Q}_b \sigma_{\alpha\mu} q_b), \end{aligned} \quad (2)$$

while the other four can be obtained by performing the charge conjugation transform to these operators:

$$\begin{aligned} J_{1\mu,R}^{(1)} &= -(\bar{q}_a \gamma_\mu Q_a)(\bar{Q}_b \gamma_5 q_b), \\ J_{2\mu,R}^{(1)} &= (\bar{q}_a \gamma_\mu \gamma_5 Q_a)(\bar{Q}_b q_b), \\ J_{3\mu,R}^{(1)} &= (\bar{q}_a \sigma_{\alpha\mu} \gamma_5 Q_a)(\bar{Q}_b \gamma^\alpha q_b), \\ J_{4\mu,R}^{(1)} &= -(\bar{q}_a \sigma_{\alpha\mu} Q_a)(\bar{Q}_b \gamma^\alpha \gamma_5 q_b). \end{aligned} \quad (3)$$

In these expressions the subscripts a and b are color indices, and q and Q represent light quarks(u, d, s) and heavy quarks(c, b), respectively.

Similarly, we can construct eight independent molecule fields belonging to $(\mathbf{8}_{[q\bar{Q}]} \otimes \mathbf{8}_{[Q\bar{q}]})$ color structure. Four of them are

$$\begin{aligned} J_{1\mu,L}^{(8)} &= (\bar{q}_a \gamma_5 \lambda_{ab}^n Q_b)(\bar{Q}_c \gamma_\mu \lambda_{cd}^n q_d), \\ J_{2\mu,L}^{(8)} &= (\bar{q}_a \lambda_{ab}^n Q_b)(\bar{Q}_c \gamma_\mu \gamma_5 \lambda_{cd}^n q_d), \\ J_{3\mu,L}^{(8)} &= (\bar{q}_a \gamma^\alpha \lambda_{ab}^n Q_b)(\bar{Q}_c \sigma_{\alpha\mu} \gamma_5 \lambda_{cd}^n q_d), \\ J_{4\mu,L}^{(8)} &= (\bar{q}_a \gamma^\alpha \gamma_5 \lambda_{ab}^n Q_b)(\bar{Q}_c \sigma_{\alpha\mu} \lambda_{cd}^n q_d), \end{aligned} \quad (4)$$

while the other four can be similarly obtained by performing the charge conjugation transform to these operators:

$$\begin{aligned} J_{1\mu,R}^{(8)} &= -(\bar{q}_a \gamma_\mu \lambda_{ab}^n Q_b)(\bar{Q}_c \gamma_5 \lambda_{cd}^n q_d), \\ J_{2\mu,R}^{(8)} &= (\bar{q}_a \gamma_\mu \gamma_5 \lambda_{ab}^n Q_b)(\bar{Q}_c \lambda_{cd}^n q_d), \\ J_{3\mu,R}^{(8)} &= (\bar{q}_a \sigma_{\alpha\mu} \gamma_5 \lambda_{ab}^n Q_b)(\bar{Q}_c \gamma^\alpha \lambda_{cd}^n q_d), \\ J_{4\mu,R}^{(8)} &= -(\bar{q}_a \sigma_{\alpha\mu} \lambda_{ab}^n Q_b)(\bar{Q}_c \gamma^\alpha \gamma_5 \lambda_{cd}^n q_d). \end{aligned} \quad (5)$$

In these expressions λ^n are eight Gell-Mann color matrices.

These 16 molecule fields with $J^P = 1^+$ in Eqs. (2)–(5) are independent, but they do not have definite charge-conjugation parities. We can use them to compose the molecular currents with definite charge-conjugation parities. The molecular currents with negative charge conjugation parity are

$$J_{i\mu}^{(1)} = J_{i\mu,L}^{(1)} - J_{i\mu,R}^{(1)}, J_{i\mu}^{(8)} = J_{i\mu,L}^{(8)} - J_{i\mu,R}^{(8)}, i = 1, \dots, 4, \quad (6)$$

and the molecular currents with positive charge conjugation parity are

$$J_{i\mu}'^{(1)} = J_{i\mu,L}^{(1)} + J_{i\mu,R}^{(1)}, J_{i\mu}'^{(8)} = J_{i\mu,L}^{(8)} + J_{i\mu,R}^{(8)}, i = 1, \dots, 4. \quad (7)$$

In this paper, we will study the Z_c states by using the molecular currents constructed in Eq. (6) with quantum numbers $J^{PC} = 1^{+-}$

$$\begin{aligned} J_{1\mu}^{(1)} &= (\bar{q}_a \gamma_5 Q_a)(\bar{Q}_b \gamma_\mu q_b) + (\bar{q}_a \gamma_\mu Q_a)(\bar{Q}_b \gamma_5 q_b), \\ J_{2\mu}^{(1)} &= (\bar{q}_a Q_a)(\bar{Q}_b \gamma_\mu \gamma_5 q_b) - (\bar{q}_a \gamma_\mu \gamma_5 Q_a)(\bar{Q}_b q_b), \\ J_{3\mu}^{(1)} &= (\bar{q}_a \gamma^\alpha Q_a)(\bar{Q}_b \sigma_{\alpha\mu} \gamma_5 q_b) - (\bar{q}_a \sigma_{\alpha\mu} \gamma_5 Q_a)(\bar{Q}_b \gamma^\alpha q_b), \\ J_{4\mu}^{(1)} &= (\bar{q}_a \gamma^\alpha \gamma_5 Q_a)(\bar{Q}_b \sigma_{\alpha\mu} q_b) + (\bar{q}_a \sigma_{\alpha\mu} Q_a)(\bar{Q}_b \gamma^\alpha \gamma_5 q_b), \\ J_{1\mu}^{(8)} &= (\bar{q}_a \gamma_5 \lambda_{ab}^n Q_b)(\bar{Q}_c \gamma_\mu \lambda_{cd}^n q_d) + (\bar{q}_a \gamma_\mu \lambda_{ab}^n Q_b)(\bar{Q}_c \gamma_5 \lambda_{cd}^n q_d), \\ J_{2\mu}^{(8)} &= (\bar{q}_a \lambda_{ab}^n Q_b)(\bar{Q}_c \gamma_\mu \gamma_5 \lambda_{cd}^n q_d) - (\bar{q}_a \gamma_\mu \gamma_5 \lambda_{ab}^n Q_b)(\bar{Q}_c \lambda_{cd}^n q_d), \\ J_{3\mu}^{(8)} &= (\bar{q}_a \gamma^\alpha \lambda_{ab}^n Q_b)(\bar{Q}_c \sigma_{\alpha\mu} \gamma_5 \lambda_{cd}^n q_d) - (\bar{q}_a \sigma_{\alpha\mu} \gamma_5 \lambda_{ab}^n Q_b)(\bar{Q}_c \gamma^\alpha \lambda_{cd}^n q_d), \\ J_{4\mu}^{(8)} &= (\bar{q}_a \gamma^\alpha \gamma_5 \lambda_{ab}^n Q_b)(\bar{Q}_c \sigma_{\alpha\mu} \lambda_{cd}^n q_d) + (\bar{q}_a \sigma_{\alpha\mu} \lambda_{ab}^n Q_b)(\bar{Q}_c \gamma^\alpha \gamma_5 \lambda_{cd}^n q_d), \end{aligned} \quad (8)$$

in which $J_{1\mu}^{(1)} - J_{4\mu}^{(1)}$ belong to the color structure $(\mathbf{1}_{[q\bar{Q}]} \otimes \mathbf{1}_{[Q\bar{q}]})$ while $J_{1\mu}^{(8)} - J_{4\mu}^{(8)}$ belong to the color structure $(\mathbf{8}_{[q\bar{Q}]} \otimes \mathbf{8}_{[Q\bar{q}]})$. The eight independent diquark-antidiquark tetraquark fields with $J^{PC} = 1^{+-}$ constructed in Ref. [35] can be written as combinations of these eight meson-meson type molecule currents. Moreover, one can construct other eight “meson-meson” type molecule currents, having the color structure $[\bar{q}_a Q_b][\bar{Q}_b q_a]$. They can also be written as combinations of these eight meson-meson type molecule currents, having the color structures $[\bar{q}_a Q_a][\bar{Q}_b q_b]$ and $[\bar{q}_a \lambda_{ab}^n Q_b][\bar{Q}_c \lambda_{cd}^n q_d]$. In general, there is no one to one correspondence between the current and the state. The independence of the currents means that if the physical state is a molecular state, it would be best to choose a molecular type of current so that it has a large overlap with the physical state. Similarly, it would be best to choose a tetraquark current for a tetraquark state.

We note that the interpolating currents listed in Eq. (8) should contain the quark contents $\bar{u}c\bar{c}u + \bar{d}c\bar{c}d$ to be neutral molecular currents of $I = 1$. Such molecular currents have quantum numbers $I^G J^{PC} = 1^+ 1^{+-}$ and thus couple to neutral Z_c states. The corresponding operators with the quark contents $\bar{u}c\bar{c}d$ or $\bar{d}c\bar{c}u$ can couple to charged Z_c states. They altogether form isospin triplets. However, we will work in the $SU(2)$ isospin symmetry without considering the effect of isospin breaking in this paper, i.e., we neglect instantons because we are in the vector channel, the masses of the up and down quarks and maintain isospin for the quark condensates $\langle \bar{u}u \rangle = \langle \bar{d}d \rangle = \langle \bar{q}q \rangle$, $\langle \bar{u}Gu \rangle = \langle \bar{d}Gd \rangle = \langle \bar{q}Gq \rangle$. Accordingly, the QCD sum rules for any iso-triplet are the same. Moreover, the isoscalar molecular currents can also be obtained from Eq. (8) with the quark contents $\bar{u}c\bar{c}u - \bar{d}c\bar{c}d$, and the sum rules for these currents are also the same as those for the isospin triplet currents. Therefore, the same mass predictions would be obtained for the neutral and charged Z_c states with $I^G J^{P(C)} = 1^+ 1^{+(-)}$ and their isoscalar partner with $I^G J^{PC} = 0^- 1^{+-}$. This expectation is reasonable for these quarkonium-like states, for example, the neutral states $Z_c^0(3900)$ [6] and $Z_c^0(4020)$ [36] lie very close to their charged partner $Z_c(3900)^+$ and $Z_c(4020)^+$, respectively.

III. QCD SUM RULES FORMALISM

With these currents constructed in Eq. (8), we can study the following two-point correlation function

$$\begin{aligned} \Pi_{\mu\nu}(q^2) &= i \int d^4x e^{iq \cdot x} \langle 0 | T [J_\mu(x) J_\nu^\dagger(0)] | 0 \rangle \\ &= \Pi(q^2) \left(\frac{q_\mu q_\nu}{q^2} - g_{\mu\nu} \right) + \Pi'(q^2) \frac{q_\mu q_\nu}{q^2}, \end{aligned} \quad (9)$$

where $\Pi(q^2)$ and $\Pi'(q^2)$ are invariant functions related to spin-1 and spin-0 states, respectively. The two-point correlation function can be described at both the hadron and quark-gluon levels. At the hadron level, the correlation function has a dispersion relation representation

$$\Pi(q^2) = \frac{(q^2)^N}{\pi} \int_{s_<}^{\infty} \frac{\text{Im}\Pi(s)}{s^N(s - q^2 - i\epsilon)} ds + \sum_{n=0}^{N-1} b_n (q^2)^n, \quad (10)$$

in which b_n are the unknown subtraction constants which can be removed by taking the Borel transform. The lower limit $s_<$ denotes a physical threshold. With this expression, one only needs to evaluate the imaginary part of the correlation function, which is much easier than the full calculation. The imaginary part of the correlation function is defined as the spectral function $\rho(s) = \frac{1}{\pi} \text{Im}\Pi(s)$, which is usually evaluated at the hadron level by inserting intermediate hadron states

$$\begin{aligned} \rho(s) &\equiv \sum_n \delta(s - m_n^2) \langle 0 | \eta | n \rangle \langle n | \eta^\dagger | 0 \rangle \\ &= f_X^2 \delta(s - m_X^2) + \text{continuum}, \end{aligned} \quad (11)$$

where we have adopted the usual pole plus continuum parametrization in the second step. All the intermediate states $|n\rangle$ must have the same quantum numbers as the interpolating currents $J_\mu(x)$. The lowest-lying resonance with hadron mass m_X couples to the current $J_\mu(x)$ via

$$\langle 0 | J_\mu | X \rangle = f_X \epsilon_\mu, \quad (12)$$

in which f_X is coupling constant and ϵ_μ is the polarization vector ($\epsilon \cdot q = 0$).

At the quark-gluon level, we evaluate the correlation function and spectral density via the QCD operator product expansion (OPE) up to dimension-eight at the leading order of α_s . The correlation function $\Pi(q^2)$ and spectral density

$\rho(s)$ can be expressed in terms of quark and gluon fields. These results are compared with Eq. (10) obtained at the hadron level to establish sum rules for hadron parameters, such as masses, magnetic moments and coupling constants of ground state hadrons. As mentioned above, we usually take Borel transform to the correlation functions at both the hadron level and quark-gluon level to remove the unknown constants in Eq. (10) and suppress the continuum contributions. Using the spectral function defined in Eq. (11), the sum rules can be obtained as

$$\mathcal{L}_k(s_0, M_B^2) = \int_{s <}^{s_0} ds e^{-s/M_B^2} \rho(s) s^k = f_X^2 m_X^{2k} e^{-m_X^2/M_B^2}, \quad (13)$$

where M_B is the Borel parameter and $\rho(s)$ in the integral is the spectral density evaluated in QCD side. The upper integral limit s_0 is the continuum threshold above which the contributions from the continuum and higher excited states can be approximated well by the spectral function. Finally, the hadron mass m_X for the lowest-lying state is extracted as

$$m_X = \sqrt{\frac{\mathcal{L}_1(s_0, M_B^2)}{\mathcal{L}_0(s_0, M_B^2)}}. \quad (14)$$

It is shown in Eqs. (13) and (14) that the extracted hadron mass m_X is a function of the continuum threshold s_0 and Borel mass M_B . One can perform the QCD sum rule analysis with these two equations. At the leading order in α_s , the spectral density $\rho(s)$ in Eq. (13) is evaluated up to dimension eight, including the perturbative term, quark condensate $\langle \bar{q}q \rangle$, gluon condensate $\langle g_s^2 GG \rangle$, quark-gluon mixed condensate $\langle \bar{q}g_s \sigma \cdot Gq \rangle$, four-quark condensate $\langle \bar{q}q \rangle^2$ and the dimension eight condensate $\langle \bar{q}q \rangle \langle \bar{q}g_s \sigma \cdot Gq \rangle$

$$\rho(s) = \rho^{\text{pert}}(s) + \rho^{\langle \bar{q}q \rangle}(s) + \rho^{\langle GG \rangle}(s) + \rho^{\langle \bar{q}q \rangle^2}(s) + \rho^{\langle \bar{q}Gq \rangle}(s) + \rho^{\langle \bar{q}q \rangle \langle \bar{q}Gq \rangle}(s). \quad (15)$$

To illustrate our numerical analysis, we use the current $J_{1\mu}^{(8)}$ as an example and show its spectral density in the following:

$$\begin{aligned} \rho_1^{(8)\text{pert}}(s) &= \frac{1}{192\pi^6} \int_{\alpha_{\min}}^{\alpha_{\max}} d\alpha \int_{\beta_{\min}}^{\beta_{\max}} d\beta \frac{(1-\alpha-\beta)(1+\alpha+\beta)[(\alpha+\beta)m_Q^2 - \alpha\beta s]^4}{\alpha^3\beta^3}, \\ \rho_1^{(8)\langle \bar{q}q \rangle}(s) &= -\frac{m_Q \langle \bar{q}q \rangle}{6\pi^4} \int_{\alpha_{\min}}^{\alpha_{\max}} d\alpha \int_{\beta_{\min}}^{\beta_{\max}} d\beta \frac{(1-\alpha-\beta)[(\alpha+\beta)m_Q^2 - \alpha\beta s][3m_Q^2(\alpha+\beta) - 7\alpha\beta s]}{\alpha\beta^2}, \\ \rho_1^{(8)\langle GG \rangle}(s) &= -\frac{\langle g_s^2 GG \rangle}{288\pi^6} \int_{\alpha_{\min}}^{\alpha_{\max}} d\alpha \int_{\beta_{\min}}^{\beta_{\max}} d\beta \left\{ \frac{7m_Q^2(1-\alpha-\beta)^2(5+\alpha+\beta)[(\alpha+\beta)m_Q^2 - \alpha\beta s]}{96\alpha^2\beta^2} \right. \\ &\quad + \frac{7m_Q^2(1+\alpha+\beta)[(\alpha+\beta)m_Q^2 - \alpha\beta s]}{16\alpha\beta} - \frac{m_Q^2(1-\alpha-\beta)^2[m_Q^2(\alpha+\beta) - 2\alpha\beta s]}{\alpha^3} \\ &\quad \left. - \frac{(1-\alpha-\beta)[m_Q^2(3+\alpha+\beta) + 2\alpha\beta s][(\alpha+\beta)m_Q^2 - \alpha\beta s]}{8\alpha^2\beta} \right\}, \\ \rho_1^{(8)\langle \bar{q}Gq \rangle}(s) &= \frac{m_Q \langle \bar{q}g_s \sigma \cdot Gq \rangle}{144\pi^4} \int_{\alpha_{\min}}^{\alpha_{\max}} d\alpha \int_{\beta_{\min}}^{\beta_{\max}} d\beta \\ &\quad \left\{ \frac{(1-\alpha-\beta)[6m_Q^2(\alpha+\beta) - 11\alpha\beta s]}{\beta^2} + \frac{17[3m_Q^2(\alpha+\beta) - 5\alpha\beta s]}{2\beta} \right\}, \\ \rho_1^{(8)\langle \bar{q}q \rangle^2}(s) &= \frac{4m_Q^2 \langle \bar{q}q \rangle^2}{9\pi^2} \sqrt{1 - 4m_Q^2/s}, \\ \rho_1^{(8)\langle \bar{q}q \rangle \langle \bar{q}Gq \rangle}(s) &= \frac{\langle \bar{q}q \rangle \langle \bar{q}g_s \sigma \cdot Gq \rangle}{108\pi^2} \int_0^1 d\alpha \left\{ \frac{24m_Q^4}{\alpha^2} \delta'(s - \tilde{m}_Q^2) + \frac{m_Q^2(5\alpha^2 - 6\alpha + 3)}{\alpha(1-\alpha)^2} \delta(s - \tilde{m}_Q^2) - \alpha H(s - \tilde{m}_Q^2) \right\}, \end{aligned} \quad (16)$$

in which $\tilde{m}_Q^2 = \frac{m_Q^2}{\alpha(1-\alpha)}$, $\delta'(s - \tilde{m}_Q^2) = \frac{d\delta(s - \tilde{m}_Q^2)}{ds}$, and $H(s - \tilde{m}_Q^2)$ is a Heaviside step function. The integration limits are $\alpha_{\min} = \frac{1 - \sqrt{1 - 4m_Q^2/s}}{2}$, $\beta_{\min} = \frac{\alpha m_Q^2}{\alpha s - m_Q^2}$, $\beta_{\max} = 1 - \alpha$, $\alpha_{\max} = \frac{1 + \sqrt{1 - 4m_Q^2/s}}{2}$ and m_Q is the heavy quark mass. We note that we have ignored the chirally suppressed terms with the light quark mass and adopted the factorization assumption of vacuum saturation for higher dimensional condensates ($D = 6$ and $D = 8$). The results for other

currents listed in Eq. (8) are collected in Appendix. A. From these expressions we can find that the $D = 3$ quark condensate $\langle \bar{q}q \rangle$ and the $D = 5$ mixed condensate $\langle \bar{q}g_s\sigma \cdot Gq \rangle$ are both multiplied by the heavy quark mass m_Q , which are thus important power corrections to the correlation functions.

IV. NUMERICAL ANALYSIS

In this section we still use the current $J_{1\mu}^{(8)}$ as an example and perform the numerical analysis. The following QCD parameters of quark masses and various condensates are used in our analysis [44–48]:

$$\begin{aligned} m_c(m_c) &= (1.23 \pm 0.09) \text{ GeV}, \\ m_b(m_b) &= (4.20 \pm 0.07) \text{ GeV}, \\ \langle \bar{q}q \rangle &= -(0.23 \pm 0.03)^3 \text{ GeV}^3, \\ \langle \bar{q}g_s\sigma \cdot Gq \rangle &= -M_0^2 \langle \bar{q}q \rangle, \\ M_0^2 &= (0.8 \pm 0.2) \text{ GeV}^2, \\ \langle g_s^2 GG \rangle &= (0.88 \pm 0.14) \text{ GeV}^4. \end{aligned} \tag{17}$$

Note that there is a minus sign implicitly included in the definition of the coupling constant g_s . We use the running masses in the \overline{MS} scheme for the charm and bottom quarks.

As mentioned above, the extracted hadron mass m_X in Eq. (14) is a function of the continuum threshold s_0 and the Borel mass M_B , which are two vital parameters in QCD sum rule analyses. If the final result, m_X , does not depend on these two free parameters, then the method of QCD sum rules would have perfect predictive power. However, reliable mass predictions are obtained when there is weak dependance on these parameters in a reasonable working regions. Principally, there are two criteria to find a Borel window (reasonable working region of M_B): the requirement of the OPE convergence results in a lower bound while the constraint of the pole contribution leads to an upper bound. At the same time, we will study the variation of the hadron mass m_X with respect to the continuum threshold. An optimized value of the continuum threshold s_0 is chosen to minimize the dependence of the extracted hadron mass m_X on the Borel mass M_B .

In Eq. (15), the non-perturbative terms are evaluated up to dimension eight. After the numerical analysis, we find that the quark condensate $\langle \bar{q}q \rangle$ and quark–gluon mixed condensate $\langle \bar{q}g_s\sigma \cdot Gq \rangle$ are dominant power corrections while the contributions of other condensates are much smaller. Using the spectral density for the current $J_{1\mu}^{(8)}$ in Eq. (17), we show the contribution of the dimension eight condensate to the correlation function $\Pi_1^{(\bar{q}q)\langle \bar{q}Gq \rangle}(M_B^2, s_0)/\Pi_1^{all}(M_B^2, s_0)$ in Fig. 1 with $s_0 \rightarrow \infty$, in which the ratio decreases with respect to M_B^2 . Accordingly, we require the dimension eight condensate contribution to be less than 5%, which results in a lower bound $M_{min}^2 = 2.8 \text{ GeV}^2$.

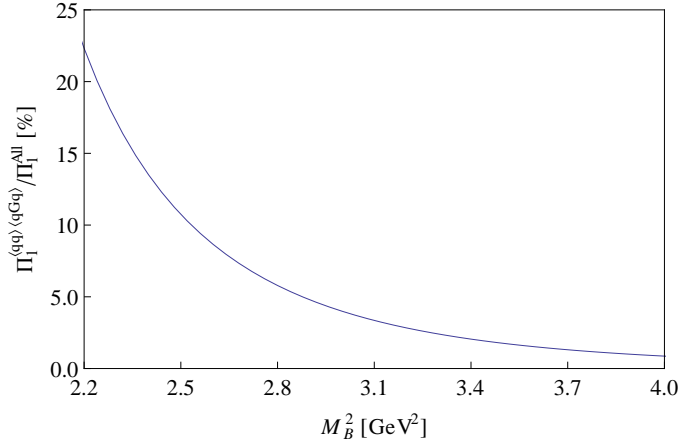


FIG. 1: OPE convergence for the current $J_{1\mu}^{(8)}$ with $s_0 \rightarrow \infty$.

To determine the upper bound on M_B^2 , we define the pole contribution(PC) using the sum rules established in Eq. (13),

$$\text{PC}(s_0, M_B^2) = \frac{\mathcal{L}_0(s_0, M_B^2)}{\mathcal{L}_0(\infty, M_B^2)}, \tag{18}$$

which represents the lowest-lying resonance contribution to the correlation function. The continuum threshold s_0 is an important parameter to the pole contribution. We study the variation of m_X with s_0 in the left panel of Fig. 2 by varying the value of M_B^2 from its lower bound. With different values of M_B^2 , there curves intersect at $s_0 = 18 \text{ GeV}^2$ around which the variation of m_X with M_B^2 reaches it minimum. This is thus an optimized value of the continuum threshold s_0 to study the pole contribution defined in Eq. (18). Requiring that PC be larger than 20%, we obtain an upper bound on the Borel mass $M_{max}^2 = 3.7 \text{ GeV}^2$. The Borel window is then determined to be $2.8 \text{ GeV}^2 \leq M_B^2 \leq 3.7 \text{ GeV}^2$ with the threshold value $s_0 = 18 \text{ GeV}^2$.

In the right panel of Fig. 2, we show the variation of the hadron mass m_X with respect to M_B^2 . The Borel window varies quickly for different value of s_0 . One notes that the mass curves decrease significantly in the region $M_B^2 \leq M_{min}^2$ while becoming quite stable inside the Borel windows. Finally, we can extract the hadron mass and the coupling constant

$$m_{X_1^{(8)}} = (3.90 \pm 0.12) \text{ GeV}, \quad (19)$$

$$f_{X_1^{(8)}} = (0.69 \pm 0.21) \times 10^{-2} \text{ GeV}^5. \quad (20)$$

This value is consistent with the mass of $Z_c(3900)$, which implies the possible molecule interpretation of this new resonance. Here we would like to emphasize that in our calculations we have not used masses of heavy-light mesons as inputs, but simply note that the obtained value 3.9 GeV (as well as other m_X listed in Table I) is close to the threshold of two heavy-light mesons. Further studies are needed to understand whether there is an underlying reason for these results.

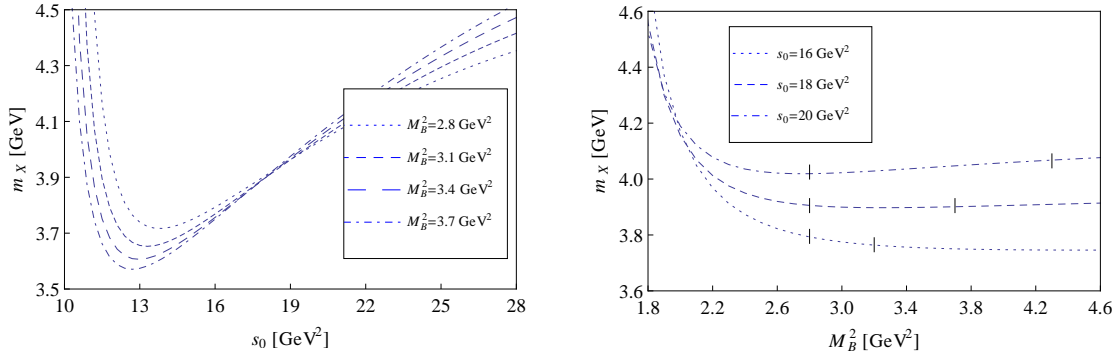


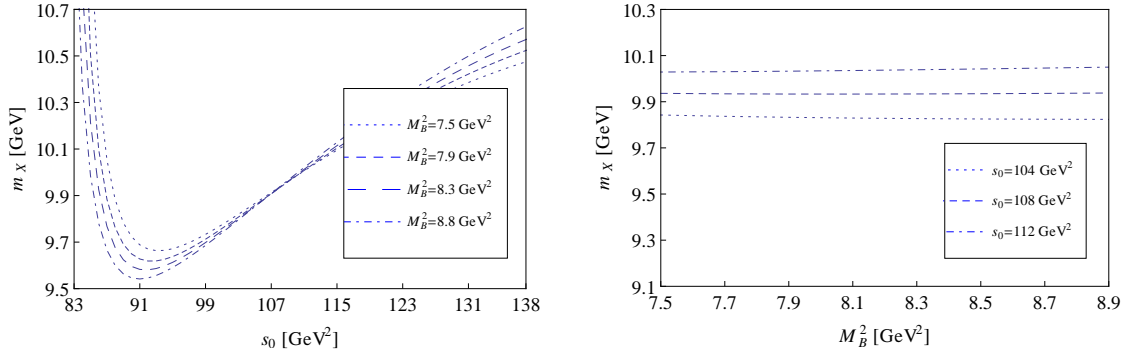
FIG. 2: Variations of the charmonium-like molecule hadron mass m_X with s_0 and M_B^2 for the current $J_{1\mu}^{(8)}$.

After performing similar numerical analyses for the other interpolating currents, we collect the extracted numerical results for the hadron masses and coupling constants in Table I. The mass sum rules for the currents $J_{2\mu}^{(1)}$ and $J_{2\mu}^{(8)}$ are unstable and thus they do not give reliable mass predictions. For the current $J_{1\mu}^{(1)}$, the lower bound of the Borel window is very small under the first (convergence) criterion. Although it leads to very good OPE convergence and broad Borel window, we need to consider the stability of the Borel curves, from which the lower bound of the Borel window is determined to be 3.3 GeV^2 . The situations for the currents $J_{4\mu}^{(1)}$ and $J_{4\mu}^{(8)}$ are very different, in which the lower bounds on M_B^2 are bigger than their upper bounds, suggesting the OPE convergence is poor for them. By loosening the criterion of the OPE convergence and requiring the dimension eight contribution to be less than 10%, we can still obtain stable mass sum rules for $J_{4\mu}^{(1)}$ and $J_{4\mu}^{(8)}$ and reliable mass predictions, as shown in Table I. The error sources including the uncertainties of the various parameters in Eq. (18) and the continuum threshold s_0 are considered to obtain the errors for hadron masses and coupling constants.

Current	$s_0(\text{GeV}^2)$	Borel window (GeV^2)	m_X (GeV)	f_X (10^{-2}GeV^5)
$J_{1\mu}^{(1)}$	21	3.3 – 4.5	4.22 ± 0.14	0.57 ± 0.16
$J_{2\mu}^{(1)}$	—	—	—	—
$J_{3\mu}^{(1)}$	20	3.3 – 4.2	4.04 ± 0.12	0.93 ± 0.27
$J_{4\mu}^{(1)}$	20	(3.0 – 3.3)	4.02 ± 0.15	0.35 ± 0.13
$J_{1\mu}^{(8)}$	18	2.8 – 3.7	3.90 ± 0.12	0.69 ± 0.21
$J_{2\mu}^{(8)}$	—	—	—	—
$J_{3\mu}^{(8)}$	18	3.1 – 3.9	3.85 ± 0.11	1.51 ± 0.46
$J_{4\mu}^{(8)}$	20	(2.8 – 3.1)	4.03 ± 0.18	0.59 ± 0.23

TABLE I: Numerical results for the charmonium-like molecule states.

In Table I, the extracted masses from the currents of color structure $(\mathbf{8}_{[q\bar{Q}]} \otimes \mathbf{8}_{[Q\bar{q}]})$ are about 3.85 – 4.03 GeV, which are slightly below the 4.02 – 4.22 GeV from the currents of color structure $(\mathbf{1}_{[q\bar{Q}]} \otimes \mathbf{1}_{[Q\bar{q}]})$, although they both lie precisely in the range of spectra of Z_c states. The masses extracted from the currents $J_{1\mu}^{(8)}$ and $J_{2\mu}^{(8)}$ are (3.90 ± 0.12) GeV and (3.85 ± 0.11) GeV respectively, which are clearly consistent with the mass of $Z_c(3900)$. The interpolating currents $J_{3\mu}^{(1)}$, $J_{4\mu}^{(1)}$ and $J_{4\mu}^{(8)}$ give hadron masses (4.04 ± 0.12) GeV, (4.02 ± 0.15) GeV and (4.03 ± 0.18) GeV respectively, which are in very close proximity to the masses of the $Z_c(4020)$ and $Z_c(4050)$ mesons, although the latter state is not confirmed to date. We note that these values are also in rough agreement with the mass of $Z_c(3900)$ state. However, one can find that it is better to chose the currents $J_{1\mu}^{(8)}$ and $J_{2\mu}^{(8)}$ to fit the mass of $Z_c(3900)$ because these two currents have a larger overlap with the physical state. We can infer that $Z_c(3900)$ has a structure well represented by the currents $J_{1\mu}^{(8)}$ and $J_{2\mu}^{(8)}$. Last but not least, the current $J_{1\mu}^{(1)}$ leads to a mass prediction (4.22 ± 0.14) GeV, which is in good agreement with the mass of $Z_c(4200)$. The interpolating currents $J_{1\mu}^{(1)}$, $J_{2\mu}^{(1)}$, $J_{3\mu}^{(1)}$ and $J_{4\mu}^{(1)}$ are constructed as $D\bar{D}^*$, $D_0^*\bar{D}_1$, $D^*\bar{D}^*$ and $D_1\bar{D}_1$ molecular operators, respectively. Our results in Table I suggest a possible landscape of hadronic molecular interpretations of the charged and neutral Z_c states. According to the above analysis, we suggest that the $Z_c(4200)$ meson to be a $D\bar{D}^*$ state, while the $Z_c(4020)$, $Z_c(4050)$ and $Z_c(3900)$ mesons to be $D^*\bar{D}^*$ or $D_1\bar{D}_1$ states. The analysis of the current $J_{2\mu}^{(1)}$ may imply that the stable $D_0^*\bar{D}_1$ molecular state does not exist.

FIG. 3: Variations of the bottomonium-like molecule hadron mass m_X with s_0 and M_B^2 for the current $J_{1\mu}^{(8)}$.

Similarly, we can study bottomonium-like molecule states with $J^{PC} = 1^{+-}$ by taking $m_Q = m_b$ in the expression of the spectral density in Eq. (17) and Appendix A. The bottomonium-like molecule system is similar to the charmonium-like system due to heavy quark symmetry. Under the same criteria, one finds that the Borel window for the $q\bar{b}b\bar{q}$ system is much broader than the $q\bar{c}c\bar{q}$ system. This suggests a stricter limitation of the pole contribution, which is only required to be larger than 20% for the $q\bar{c}c\bar{q}$ systems. For the $q\bar{b}b\bar{q}$ system with $J_{1\mu}^{(8)}$, we require the same OPE convergence criterion as the $q\bar{c}c\bar{q}$ system while modifying the requirement of the pole contribution to be larger than 30%. The Borel window is obtained as $7.5\text{ GeV}^2 \leq M_B^2 \leq 8.8\text{ GeV}^2$ with the continuum threshold $s_0 = 108\text{ GeV}^2$. Using these values of the parameters, we show the variations of the hadron mass with respect to the Borel mass M_B^2 and the threshold value s_0 in Fig. 3. The Borel curves are shown to be very stable and give reliable predictions of the

hadron mass and coupling constant

$$m_{X_{1b}^{(8)}} = (9.93 \pm 0.15) \text{ GeV}, \quad (21)$$

$$f_{X_{1b}^{(8)}} = (1.02 \pm 0.30) \times 10^{-3} \text{ GeV}^5. \quad (22)$$

After numerical analyses of all interpolating currents, we collect the numerical results for the $q\bar{b}b\bar{q}$ states in Table II. Similar to the charmonium-like system, there is no significant Borel window for the current $J_{4\mu}^{(8)}$ under the above criteria. The Borel window $(7.5 - 8.5) \text{ GeV}^2$ written in parenthesis is obtained by loosening the requirement of the OPE convergence to be 10%. However, the mass prediction under this Borel window is still reliable. The extracted mass for the current $J_{1\mu}^{(1)}$ is about $10.48 \pm 0.15 \text{ GeV}$, which is consistent with the mass of the $Z_b(10610)$ meson within the error, supporting the $B\bar{B}^*$ molecule interpretation for this state.

Current	$s_0(\text{GeV}^2)$	Borel window (GeV^2)	m_X (GeV)	f_X (10^{-3}GeV^5)
$J_{1\mu}^{(1)}$	121	8.0 – 11.0	10.48 ± 0.15	1.45 ± 0.19
$J_{2\mu}^{(1)}$	—	—	—	—
$J_{3\mu}^{(1)}$	113	8.0 – 9.4	10.14 ± 0.15	1.69 ± 0.46
$J_{4\mu}^{(1)}$	117	7.5 – 8.3	10.33 ± 0.14	0.58 ± 0.34
$J_{1\mu}^{(8)}$	108	7.5 – 8.8	9.93 ± 0.15	1.02 ± 0.30
$J_{2\mu}^{(8)}$	—	—	—	—
$J_{3\mu}^{(8)}$	108	7.8 – 8.7	9.92 ± 0.15	2.17 ± 0.62
$J_{4\mu}^{(8)}$	119	(7.5 – 8.5)	10.46 ± 0.14	1.67 ± 0.55

TABLE II: Numerical results for the bottomonium-like molecule states.

V. SUMMARY AND DISCUSSIONS

To study the charged exotic Z_c and Z_b states, we constructed all the charmonium-like/bottomonium-like molecular interpolating currents with $J^{PC} = 1^{+-}$, including both the singlet-singlet and octet-octet types of color structures. We calculated the two-point correlation functions and spectral densities for these $q\bar{Q}Q\bar{q}$ operators. Within the $SU(2)$ isospin symmetry, all the numerical results of hadron masses and coupling constants in Tables I and II are suitable for the neutral and charged Z_c states with $I^G J^{P(C)} = 1^+ 1^{+(-)}$ and their isoscalar partner with $I^G J^{PC} = 0^- 1^{+-}$.

At the leading order in α_s , we calculated the two-point correlation functions and spectral densities up to dimension eight, including the perturbative term, the quark condensate $\langle\bar{q}q\rangle$, the mixed condensate $\langle\bar{q}g_s\sigma \cdot Gq\rangle$, the gluon condensate $\langle g_s^2 GG\rangle$, the four-quark condensate $\langle\bar{q}q\rangle^2$ and the $D = 8$ condensate $\langle\bar{q}q\rangle\langle\bar{q}g_s\sigma \cdot Gq\rangle$. Being proportional to the heavy quark mass, the quark condensate $\langle\bar{q}q\rangle$ is the dominant power correction to the correlation function while the mixed condensate $\langle\bar{q}g_s\sigma \cdot Gq\rangle$ also gives an important contribution. After performing the numerical analyses, we obtain reliable mass predictions $4.02 - 4.22 \text{ GeV}$ for the color singlet-singlet charmonium-like molecular states and $3.85 - 4.03 \text{ GeV}$ for the color octet-octet ones. This mass spectrum of the $q\bar{c}c\bar{q}$ states is precisely consistent with the masses of the Z_c states, suggesting a possible landscape of hadronic molecular interpretations of the newly observed Z_c states. We suggest that the $Z_c(4200)$ meson is a $D\bar{D}^*$ state while the $Z_c(4020)$, $Z_c(4050)$ and $Z_c(3900)$ mesons is either a $D^*\bar{D}^*$ or $D_1\bar{D}_1$ state. The stable $D_0^*\bar{D}_1$ molecular state does not occur in our result.

The bottomonium-like $q\bar{b}b\bar{q}$ molecular states are also studied and the numerical results are collected in Table II. The extracted masses are predicted to be around $9.92 - 10.48 \text{ GeV}$, which are slightly lower than the masses of the charged $Z_b(10610)$ meson. However, the charged $Z_b(10610)$ meson is consistent with a $B\bar{B}^*$ molecular state within the theoretical uncertainties.

One finds that the hadron masses extracted from the color singlet-singlet currents are a bit higher than those extracted from the color octet-octet currents, for both the charmonium-like and bottomonium-like systems. This situation is different from the result in Ref. [49], in which the color octet-octet tetraquarks were heavier. In Refs. [50, 51], the color-octet mechanism was found to give contributions to quarkonia production via the emission or absorption of a soft gluon in NRQCD. Similar mechanisms can be expected in the octet-octet quarkonium-like molecular systems, in which a color-octet $Q\bar{q}$ pair combines with another color-octet $Q\bar{Q}$ pair by exchanging a gluon.

The possible hadronic decay patterns of the $q\bar{c}c\bar{q}$ and $q\bar{b}b\bar{q}$ molecular states can be discussed by considering the kinematic constraints and the conversations of parity, C-parity, isospin and G-parity. Considering the hadron masses

obtained in Table I, the possible S-wave two-meson hadronic decay channels for the charmonium-like $q\bar{c}c\bar{q}$ molecular states with $I^G J^{P(C)} = 1^+ 1^{+(-)}$ are

$$Z_c \rightarrow D\bar{D}^*, D^*\bar{D}^*, \eta_c(1S)\rho, J/\psi\pi, \psi(2S)\pi, \quad (23)$$

and the possible P-wave decay channels are

$$Z_c \rightarrow D_0^*\bar{D}, \eta_c(1S)b_1((1235)). \quad (24)$$

For their isoscalar $q\bar{c}c\bar{q}$ partners with $I^G J^{PC} = 0^- 1^{+-}$, the possible S-wave decay channels are

$$Z_c \rightarrow D\bar{D}^*, D^*\bar{D}^*, \eta_c(1S)\omega, J/\psi\eta, J/\psi\eta', \quad (25)$$

while the P-wave decay channels are

$$Z_c \rightarrow \eta_c(1S)h_1(1170), J/\psi f_0(980), J/\psi a_0(980), h_c(1P)\eta. \quad (26)$$

For the bottomonium-like $q\bar{b}b\bar{q}$ molecular states, the extracted masses in Table II lie below the open-bottom thresholds so that only the hidden-flavor decay channels are kinematically allowed. The possible S-wave decay patterns for the $q\bar{b}b\bar{q}$ states with $I^G J^{P(C)} = 1^+ 1^{+(-)}$ are $Z_b \rightarrow \Upsilon(1S)\pi, \Upsilon(2S)\pi$ while the S-wave decays are forbidden. For the isoscalar partners with $I^G J^{PC} = 0^- 1^{+-}$, their possible S-wave and P-wave decay channels are $Z_b \rightarrow \Upsilon(1S)\eta$ and $Z_b \rightarrow \Upsilon(1S)f_0(980), \Upsilon(1S)a_0(980)$, respectively.

Acknowledgments

This project is supported by the Natural Sciences and Engineering Research Council of Canada (NSERC). H.X.C and S.L.Z. are supported by the National Natural Science Foundation of China under Grants No. 11205011, No. 11475015, and No. 11261130311.

-
- [1] S. K. Choi et al. (BELLE), Phys. Rev. Lett. **100**, 142001 (2008).
 - [2] R. Aaij et al. (LHCb collaboration), Phys.Rev.Lett. **112**, 222002 (2014).
 - [3] R. Mizuk et al. (Belle collaboration), Phys. Rev. **D78**, 072004 (2008).
 - [4] M. Ablikim et al. (BESIII Collaboration), Phys.Rev.Lett. **110**, 252001 (2013).
 - [5] Z. Liu et al. (Belle Collaboration), Phys.Rev.Lett. **110**, 252002 (2013).
 - [6] T. Xiao, S. Dobbs, A. Tomaradze, and K. K. Seth, Phys.Lett. **B727**, 366 (2013).
 - [7] M. Ablikim et al. (BESIII Collaboration), Phys.Rev.Lett. **111**, 242001 (2013).
 - [8] M. Ablikim et al. (BESIII Collaboration), Phys.Rev.Lett. **112**, 132001 (2014).
 - [9] K. Chilikin et al. (Belle Collaboration), Phys.Rev. **D90**, 112009 (2014).
 - [10] X. Wang, C. Yuan, C. Shen, P. Wang, A. Abdesselam, et al. (2014), arXiv:1410.7641.
 - [11] I. Adachi (Belle Collaboration) (2011), arXiv:1105.4583.
 - [12] A. Esposito, A. L. Guerrieri, F. Piccinini, A. Pilloni, and A. D. Polosa, Int.J.Mod.Phys. **A30**, 1530002 (2015).
 - [13] S. L. Olsen, Front.Phys. **10**, 101401 (2015).
 - [14] X. Liu, Chin. Sci. Bull. **59**, 3815 (2014).
 - [15] Q. Wang, C. Hanhart, and Q. Zhao, Phys.Rev.Lett. **111**, 132003 (2013).
 - [16] F. Aceti, M. Bayar, E. Oset, A. M. Torres, K. Khemchandani, et al., Phys.Rev. **D90**, 016003 (2014).
 - [17] L. Zhao, L. Ma, and S.-L. Zhu, Phys.Rev. **D89**, 094026 (2014).
 - [18] W. Chen, T. Steele, M.-L. Du, and S.-L. Zhu, Eur.Phys.J. **C74**, 2773 (2014).
 - [19] X. Wang, Y. Sun, D.-Y. Chen, X. Liu, and T. Matsuki, Eur.Phys.J. **C74**, 2761 (2014).
 - [20] C.-Y. Cui, Y.-L. Liu, and M.-Q. Huang (2013), arXiv:1308.3625.
 - [21] L. Zhao, W.-Z. Deng, and S.-L. Zhu, Phys.Rev. **D90**, 094031 (2014).
 - [22] W. Chen, T. Steele, H.-X. Chen, and S.-L. Zhu (2015), arXiv:1501.03863.
 - [23] Z.-G. Wang (2015), 1502.01459.
 - [24] M. E. Bracco, S. H. Lee, M. Nielsen, and R. Rodrigues da Silva, Phys. Lett. **B671**, 240 (2009).
 - [25] L. Maiani, A. D. Polosa, and V. Riquer, New J. Phys. **10**, 073004 (2008).
 - [26] L. Maiani, F. Piccinini, A. Polosa, and V. Riquer, Phys.Rev. **D89**, 114010 (2014).
 - [27] S. H. Lee, A. Mihara, F. S. Navarra, and M. Nielsen, Phys. Lett. **B661**, 28 (2008).
 - [28] C. Meng and K.-T. Chao (2007), arXiv:0708.4222.
 - [29] G.-J. Ding (2007), arXiv:0711.1485.

- [30] J.-R. Zhang, M. Zhong, and M.-Q. Huang, Phys.Lett. **B704**, 312 (2011).
- [31] Z.-F. Sun, J. He, X. Liu, Z.-G. Luo, and S.-L. Zhu, Phys.Rev. **D84**, 054002 (2011).
- [32] D. Ebert, R. N. Faustov, and V. O. Galkin, Phys. Lett. **B634**, 214 (2006), hep-ph/0512230.
- [33] D. Ebert, R. Faustov, V. Galkin, and W. Lucha, Phys.Rev. **D76**, 114015 (2007).
- [34] W. Chen and S.-L. Zhu, Phys.Rev. **D81**, 105018 (2010).
- [35] W. Chen and S.-L. Zhu, Phys. Rev. **D83**, 034010 (2011).
- [36] M. Ablikim et al. (BESIII Collaboration), Phys.Rev.Lett. **113**, 212002 (2014).
- [37] M.-L. Du, W. Chen, X.-L. Chen, and S.-L. Zhu, Chin.Phys. **C37**, 033104 (2013).
- [38] M. A. Shifman, A. I. Vainshtein, and V. I. Zakharov, Nucl. Phys. **B147**, 385 (1979).
- [39] L. J. Reinders, H. Rubinstein, and S. Yazaki, Phys. Rept. **127**, 1 (1985).
- [40] P. Colangelo and A. Khodjamirian, Frontier of Particle Physics **3** (2000), hep-ph/0010175.
- [41] D. Jido, N. Kodama and M. Oka, Phys. Rev. D **54**, 4532 (1996).
- [42] Y. Kondo, O. Morimatsu and T. Nishikawa, Nucl. Phys. A **764**, 303 (2006).
- [43] K. Ohtani, P. Gubler and M. Oka, Phys. Rev. D **87**, no. 3, 034027 (2013).
- [44] K. Olive et al. (Particle Data Group), Chin.Phys. **C38**, 090001 (2014).
- [45] M. Eidemuller and M. Jamin, Phys. Lett. **B498**, 203 (2001), hep-ph/0010334.
- [46] M. Jamin and A. Pich, Nucl. Phys. Proc. Suppl. **74**, 300 (1999), hep-ph/9810259.
- [47] M. Jamin, J. A. Oller, and A. Pich, Eur. Phys. J. **C24**, 237 (2002), hep-ph/0110194.
- [48] A. Khodjamirian, T. Mannel, N. Offen, and Y.-M. Wang, Phys.Rev. **D83**, 094031 (2011).
- [49] Zhi-Gang Wang, and Tao Huang, Eur. Phys. J. **C74**, 2891 (2014).
- [50] P. L. Cho, and A. K. Leibovich, Phys.Rev. **D53**, 150 (1996).
- [51] E. Braaten, and Y.-Q. Chen, Phys.Rev.Lett. **76**, 730 (1996).

Appendix A: Expressions of spectral density for other interpolating currents

In Eq. (17), we have given the spectral density extracted from the current $J_{1\mu}^{(8)}$. For other interpolating currents listed in Eq. (8), we collect the expressions of the spectral density in this appendix up to dimension eight condensate, as shown in (15).

- For the current $J_{1\mu}^{(1)}$

$$\begin{aligned}
 \rho_1^{(1)pert}(s) &= \frac{3}{2048\pi^6} \int_{\alpha_{min}}^{\alpha_{max}} d\alpha \int_{\beta_{min}}^{\beta_{max}} d\beta \frac{(1-\alpha-\beta)(1+\alpha+\beta) [(\alpha+\beta)m_Q^2 - \alpha\beta s]^4}{\alpha^3\beta^3}, \\
 \rho_1^{(1)\langle\bar{q}q\rangle}(s) &= -\frac{3m_Q\langle\bar{q}q\rangle}{64\pi^4} \int_{\alpha_{min}}^{\alpha_{max}} d\alpha \int_{\beta_{min}}^{\beta_{max}} d\beta \frac{(1-\alpha-\beta) [(\alpha+\beta)m_Q^2 - \alpha\beta s] [3m_Q^2(\alpha+\beta) - 7\alpha\beta s]}{\alpha\beta^2}, \\
 \rho_1^{(1)\langle GG\rangle}(s) &= -\frac{\langle g_s^2 GG\rangle}{512\pi^6} \int_{\alpha_{min}}^{\alpha_{max}} d\alpha \int_{\beta_{min}}^{\beta_{max}} d\beta \\
 &\quad \left\{ \frac{(1-\alpha-\beta) [(\alpha+\beta)m_Q^2 - \alpha\beta s] s}{\alpha} - \frac{m_Q^2(1-\alpha-\beta)^2 [m_Q^2(\alpha+\beta) - 2\alpha\beta s]}{2\alpha^3} \right\}, \\
 \rho_1^{(1)\langle\bar{q}Gq\rangle}(s) &= -\frac{3m_Q\langle\bar{q}g_s\sigma \cdot Gq\rangle}{64\pi^4} \int_{\alpha_{min}}^{\alpha_{max}} d\alpha \int_{\beta_{min}}^{\beta_{max}} d\beta \\
 &\quad \left\{ \frac{(1-\alpha-\beta) [m_Q^2(\alpha+\beta) - 2\alpha\beta s]}{\beta^2} - \frac{7m_Q^2(\alpha+\beta) - 11\alpha\beta s}{2\alpha\beta} \right\}, \\
 \rho_1^{(1)\langle\bar{q}q\rangle^2}(s) &= \frac{m_Q^2\langle\bar{q}q\rangle^2}{8\pi^2} \sqrt{1 - 4m_Q^2/s}, \\
 \rho_1^{(1)\langle\bar{q}q\rangle\langle\bar{q}Gq\rangle}(s) &= \frac{\langle\bar{q}q\rangle\langle\bar{q}g_s\sigma \cdot Gq\rangle}{16\pi^2} \int_0^1 d\alpha \left\{ \frac{m_Q^4}{\alpha^2} \delta'(s - \tilde{m}_Q^2) - \frac{m_Q^2}{\alpha} \delta(s - \tilde{m}_Q^2) \right\}. \tag{A1}
 \end{aligned}$$

- For the current $J_{2\mu}^{(1)}$

$$\rho_2^{(1)pert}(s) = \frac{3}{2048\pi^6} \int_{\alpha_{min}}^{\alpha_{max}} d\alpha \int_{\beta_{min}}^{\beta_{max}} d\beta \frac{(1-\alpha-\beta)(1+\alpha+\beta) [(\alpha+\beta)m_Q^2 - \alpha\beta s]^4}{\alpha^3\beta^3},$$

$$\begin{aligned}
\rho_2^{(1)\langle\bar{q}q\rangle}(s) &= \frac{3m_Q\langle\bar{q}q\rangle}{64\pi^4} \int_{\alpha_{min}}^{\alpha_{max}} d\alpha \int_{\beta_{min}}^{\beta_{max}} d\beta \frac{(1-\alpha-\beta)[(\alpha+\beta)m_Q^2-\alpha\beta s][3m_Q^2(\alpha+\beta)-7\alpha\beta s]}{\alpha\beta^2}, \\
\rho_2^{(1)\langle GG\rangle}(s) &= -\frac{\langle g_s^2 GG\rangle}{512\pi^6} \int_{\alpha_{min}}^{\alpha_{max}} d\alpha \int_{\beta_{min}}^{\beta_{max}} d\beta \\
&\quad \left\{ \frac{(1-\alpha-\beta)[(\alpha+\beta)m_Q^2-\alpha\beta s]s}{\alpha} - \frac{m_Q^2(1-\alpha-\beta)^2[m_Q^2(\alpha+\beta)-2\alpha\beta s]}{2\alpha^3} \right\}, \\
\rho_2^{(1)\langle\bar{q}Gq\rangle}(s) &= \frac{3m_Q\langle\bar{q}g_s\sigma\cdot Gq\rangle}{64\pi^4} \int_{\alpha_{min}}^{\alpha_{max}} d\alpha \int_{\beta_{min}}^{\beta_{max}} d\beta \\
&\quad \left\{ \frac{(1-\alpha-\beta)[m_Q^2(\alpha+\beta)-2\alpha\beta s]}{\beta^2} - \frac{7m_Q^2(\alpha+\beta)-11\alpha\beta s}{2\alpha\beta} \right\}, \\
\rho_2^{(1)\langle\bar{q}q\rangle^2}(s) &= \frac{m_Q^2\langle\bar{q}q\rangle^2}{8\pi^2} \sqrt{1-4m_Q^2/s}, \\
\rho_2^{(1)\langle\bar{q}q\rangle\langle\bar{q}Gq\rangle}(s) &= \frac{\langle\bar{q}q\rangle\langle\bar{q}g_s\sigma\cdot Gq\rangle}{16\pi^2} \int_0^1 d\alpha \left\{ \frac{m_Q^4}{\alpha^2} \delta'(s-\tilde{m}_Q^2) - \frac{m_Q^2}{\alpha} \delta(s-\tilde{m}_Q^2) \right\}. \tag{A2}
\end{aligned}$$

- For the current $J_{3\mu}^{(1)}$

$$\begin{aligned}
\rho_3^{(1)pert}(s) &= \frac{1}{512\pi^6} \int_{\alpha_{min}}^{\alpha_{max}} d\alpha \int_{\beta_{min}}^{\beta_{max}} d\beta \left\{ \frac{9(1-\alpha-\beta)(1+\alpha+\beta)[(\alpha+\beta)m_Q^2-\alpha\beta s]^4}{4\alpha^3\beta^3} \right. \\
&\quad \left. - \frac{m_Q^2(1-\alpha-\beta)^2(5+\alpha+\beta)[(\alpha+\beta)m_Q^2-\alpha\beta s]^3}{\alpha^3\beta^3} \right\}, \\
\rho_3^{(1)\langle\bar{q}q\rangle}(s) &= -\frac{9m_Q\langle\bar{q}q\rangle}{64\pi^4} \int_{\alpha_{min}}^{\alpha_{max}} d\alpha \int_{\beta_{min}}^{\beta_{max}} d\beta \frac{(1-\alpha-\beta)[(\alpha+\beta)m_Q^2-\alpha\beta s][3m_Q^2(\alpha+\beta)-7\alpha\beta s]}{\alpha\beta^2}, \\
\rho_3^{(1)\langle GG\rangle}(s) &= \frac{\langle g_s^2 GG\rangle}{1024\pi^6} \int_{\alpha_{min}}^{\alpha_{max}} d\alpha \int_{\beta_{min}}^{\beta_{max}} d\beta \left\{ \frac{3m_Q^2(1-\alpha-\beta)^2[m_Q^2(\alpha+\beta)-2\alpha\beta s]}{\alpha^3} \right. \\
&\quad - \frac{m_Q^2(1-\alpha-\beta)^2(5+\alpha+\beta)\{3(\alpha^2+\beta^2)[(\alpha+\beta)m_Q^2-\alpha\beta s]+m_Q^2(\alpha^3+\beta^3)\}}{6\alpha^3\beta^3} \\
&\quad \left. + \frac{(1-\alpha-\beta)[(\alpha+\beta)m_Q^2-\alpha\beta s][m_Q^2(3+\alpha+\beta)+2\alpha\beta s]}{\alpha^2\beta} \right\}, \\
\rho_3^{(1)\langle\bar{q}Gq\rangle}(s) &= \frac{m_Q\langle\bar{q}g_s\sigma\cdot Gq\rangle}{64\pi^4} \int_{\alpha_{min}}^{\alpha_{max}} d\alpha \int_{\beta_{min}}^{\beta_{max}} d\beta \\
&\quad \left\{ \frac{(1-\alpha-\beta)[3m_Q^2(\alpha+\beta)-4\alpha\beta s]}{\beta^2} + \frac{(2+7\alpha-2\beta)[3m_Q^2(\alpha+\beta)-5\alpha\beta s]}{2\alpha\beta} \right\}, \\
\rho_3^{(1)\langle\bar{q}q\rangle^2}(s) &= \frac{5(2m_Q^2+s)\langle\bar{q}q\rangle^2}{48\pi^2} \sqrt{1-4m_Q^2/s}, \\
\rho_3^{(1)\langle\bar{q}q\rangle\langle\bar{q}Gq\rangle}(s) &= \frac{\langle\bar{q}q\rangle\langle\bar{q}g_s\sigma\cdot Gq\rangle}{48\pi^2} \int_0^1 d\alpha \left\{ \frac{3m_Q^4(3-\alpha)}{(1-\alpha)\alpha^2} \delta'(s-\tilde{m}_Q^2) \right. \\
&\quad \left. + \frac{m_Q^2(3\alpha^3-4\alpha^2-3\alpha+6)}{\alpha(1-\alpha)^2} \delta(s-\tilde{m}_Q^2) + (2\alpha+3)H(s-\tilde{m}_Q^2) \right\}. \tag{A3}
\end{aligned}$$

- For the current $J_{4\mu}^{(1)}$

$$\rho_4^{(1)pert}(s) = \frac{1}{512\pi^6} \int_{\alpha_{min}}^{\alpha_{max}} d\alpha \int_{\beta_{min}}^{\beta_{max}} d\beta \left\{ \frac{9(1-\alpha-\beta)(1+\alpha+\beta)[(\alpha+\beta)m_Q^2-\alpha\beta s]^4}{4\alpha^3\beta^3} \right.$$

$$\begin{aligned}
& - \frac{m_Q^2(1-\alpha-\beta)^2(5+\alpha+\beta)[(\alpha+\beta)m_Q^2-\alpha\beta s]^3}{\alpha^3\beta^3} \Big\}, \\
\rho_4^{(1)\langle\bar{q}q\rangle}(s) &= \frac{9m_Q\langle\bar{q}q\rangle}{64\pi^4} \int_{\alpha_{min}}^{\alpha_{max}} d\alpha \int_{\beta_{min}}^{\beta_{max}} d\beta \frac{(1-\alpha-\beta)[(\alpha+\beta)m_Q^2-\alpha\beta s][3m_Q^2(\alpha+\beta)-7\alpha\beta s]}{\alpha\beta^2}, \\
\rho_4^{(1)\langle GG\rangle}(s) &= \frac{\langle g_s^2 GG\rangle}{1024\pi^6} \int_{\alpha_{min}}^{\alpha_{max}} d\alpha \int_{\beta_{min}}^{\beta_{max}} d\beta \left\{ \frac{3m_Q^2(1-\alpha-\beta)^2[m_Q^2(\alpha+\beta)-2\alpha\beta s]}{\alpha^3} \right. \\
& \quad - \frac{m_Q^2(1-\alpha-\beta)^2(5+\alpha+\beta)\{3(\alpha^2+\beta^2)[(\alpha+\beta)m_Q^2-\alpha\beta s]+m_Q^2(\alpha^3+\beta^3)\}}{6\alpha^3\beta^3} \\
& \quad \left. + \frac{(1-\alpha-\beta)[(\alpha+\beta)m_Q^2-\alpha\beta s][m_Q^2(3+\alpha+\beta)+2\alpha\beta s]}{\alpha^2\beta} \right\}, \\
\rho_4^{(1)\langle\bar{q}Gq\rangle}(s) &= -\frac{m_Q\langle\bar{q}g_s\sigma\cdot Gq\rangle}{64\pi^4} \int_{\alpha_{min}}^{\alpha_{max}} d\alpha \int_{\beta_{min}}^{\beta_{max}} d\beta \\
& \quad \left\{ \frac{(1-\alpha-\beta)[3m_Q^2(\alpha+\beta)-4\alpha\beta s]}{\beta^2} + \frac{(2+7\alpha-2\beta)[3m_Q^2(\alpha+\beta)-5\alpha\beta s]}{2\alpha\beta} \right\}, \\
\rho_4^{(1)\langle\bar{q}q\rangle^2}(s) &= \frac{5(2m_Q^2+s)\langle\bar{q}q\rangle^2}{48\pi^2} \sqrt{1-4m_Q^2/s}, \\
\rho_4^{(1)\langle\bar{q}q\rangle\langle\bar{q}Gq\rangle}(s) &= \frac{\langle\bar{q}q\rangle\langle\bar{q}g_s\sigma\cdot Gq\rangle}{48\pi^2} \int_0^1 d\alpha \left\{ \frac{3m_Q^4(3-\alpha)}{(1-\alpha)\alpha^2} \delta'(s-\tilde{m}_Q^2) \right. \\
& \quad \left. + \frac{m_Q^2(3\alpha^3-4\alpha^2-3\alpha+6)}{\alpha(1-\alpha)^2} \delta(s-\tilde{m}_Q^2) + (2\alpha+3)H(s-\tilde{m}_Q^2) \right\}. \tag{A4}
\end{aligned}$$

• For the current $J_{2\mu}^{(8)}$

$$\begin{aligned}
\rho_2^{(8)pert}(s) &= \frac{1}{192\pi^6} \int_{\alpha_{min}}^{\alpha_{max}} d\alpha \int_{\beta_{min}}^{\beta_{max}} d\beta \frac{(1-\alpha-\beta)(1+\alpha+\beta)[(\alpha+\beta)m_Q^2-\alpha\beta s]^4}{\alpha^3\beta^3}, \\
\rho_2^{(8)\langle\bar{q}q\rangle}(s) &= \frac{m_Q\langle\bar{q}q\rangle}{6\pi^4} \int_{\alpha_{min}}^{\alpha_{max}} d\alpha \int_{\beta_{min}}^{\beta_{max}} d\beta \frac{(1-\alpha-\beta)[(\alpha+\beta)m_Q^2-\alpha\beta s][3m_Q^2(\alpha+\beta)-7\alpha\beta s]}{\alpha\beta^2}, \\
\rho_2^{(8)\langle GG\rangle}(s) &= -\frac{\langle g_s^2 GG\rangle}{288\pi^6} \int_{\alpha_{min}}^{\alpha_{max}} d\alpha \int_{\beta_{min}}^{\beta_{max}} d\beta \left\{ \frac{7m_Q^2(1-\alpha-\beta)^2(5+\alpha+\beta)[(\alpha+\beta)m_Q^2-\alpha\beta s]}{96\alpha^2\beta^2} \right. \\
& \quad + \frac{7m_Q^2(1+\alpha+\beta)[(\alpha+\beta)m_Q^2-\alpha\beta s]}{16\alpha\beta} - \frac{m_Q^2(1-\alpha-\beta)^2[m_Q^2(\alpha+\beta)-2\alpha\beta s]}{\alpha^3} \\
& \quad \left. - \frac{(1-\alpha-\beta)[m_Q^2(3+\alpha+\beta)+2\alpha\beta s][(\alpha+\beta)m_Q^2-\alpha\beta s]}{8\alpha^2\beta} \right\}, \\
\rho_2^{(8)\langle\bar{q}Gq\rangle}(s) &= -\frac{m_Q\langle\bar{q}g_s\sigma\cdot Gq\rangle}{144\pi^4} \int_{\alpha_{min}}^{\alpha_{max}} d\alpha \int_{\beta_{min}}^{\beta_{max}} d\beta \\
& \quad \left\{ \frac{(1-\alpha-\beta)[6m_Q^2(\alpha+\beta)-11\alpha\beta s]}{\beta^2} + \frac{17[3m_Q^2(\alpha+\beta)-5\alpha\beta s]}{2\beta} \right\}, \tag{A5} \\
\rho_2^{(8)\langle\bar{q}q\rangle^2}(s) &= \frac{4m_Q^2\langle\bar{q}q\rangle^2}{9\pi^2} \sqrt{1-4m_Q^2/s}, \\
\rho_2^{(8)\langle\bar{q}q\rangle\langle\bar{q}Gq\rangle}(s) &= \frac{\langle\bar{q}q\rangle\langle\bar{q}g_s\sigma\cdot Gq\rangle}{108\pi^2} \int_0^1 d\alpha \left\{ \frac{24m_Q^4}{\alpha^2} \delta'(s-\tilde{m}_Q^2) + \frac{m_Q^2(5\alpha^2-6\alpha+3)}{\alpha(1-\alpha)^2} \delta(s-\tilde{m}_Q^2) - \alpha H(s-\tilde{m}_Q^2) \right\}.
\end{aligned}$$

- For the current $J_{3\mu}^{(8)}$

$$\begin{aligned}
\rho_3^{(8)pert}(s) &= \frac{1}{16\pi^6} \int_{\alpha_{min}}^{\alpha_{max}} d\alpha \int_{\beta_{min}}^{\beta_{max}} d\beta \left\{ \frac{(1-\alpha-\beta)(1+\alpha+\beta) [(\alpha+\beta)m_Q^2 - \alpha\beta s]^4}{4\alpha^3\beta^3} \right. \\
&\quad \left. - \frac{m_Q^2(1-\alpha-\beta)^2(5+\alpha+\beta) [(\alpha+\beta)m_Q^2 - \alpha\beta s]^3}{9\alpha^3\beta^3} \right\}, \\
\rho_3^{(8)\langle\bar{q}q\rangle}(s) &= -\frac{m_Q\langle\bar{q}q\rangle}{2\pi^4} \int_{\alpha_{min}}^{\alpha_{max}} d\alpha \int_{\beta_{min}}^{\beta_{max}} d\beta \frac{(1-\alpha-\beta) [(\alpha+\beta)m_Q^2 - \alpha\beta s] [3m_Q^2(\alpha+\beta) - 7\alpha\beta s]}{\alpha\beta^2}, \\
\rho_3^{(8)\langle GG\rangle}(s) &= -\frac{\langle g_s^2 GG\rangle}{96\pi^6} \int_{\alpha_{min}}^{\alpha_{max}} d\alpha \int_{\beta_{min}}^{\beta_{max}} d\beta \left\{ \frac{m_Q^2(1-\alpha-\beta)^2(5+\alpha+\beta) [m_Q^2(3\alpha+4\beta) - 3\alpha\beta s]}{9\alpha^3\beta} \right. \\
&\quad + \frac{7(1-\alpha-\beta)^2 [(\alpha+\beta)m_Q^2 - \alpha\beta s] [m_Q^2(13\alpha+13\beta+29) + 12\alpha\beta s]}{288\alpha^2\beta^2} \\
&\quad - \frac{m_Q^2(1-\alpha-\beta)^2 [m_Q^2(\alpha+\beta) - 2\alpha\beta s]}{\alpha^3} \\
&\quad + \frac{7 [(\alpha+\beta)m_Q^2 - \alpha\beta s] [3m_Q^2(1+\alpha+\beta) + 4\alpha\beta s]}{48\alpha\beta} \\
&\quad \left. + \frac{(1-\alpha-\beta) [(\alpha+\beta)m_Q^2 - \alpha\beta s] [m_Q^2(3+\alpha+\beta) + 5\alpha\beta s]}{12\alpha^2\beta} \right\}, \\
\rho_3^{(8)\langle\bar{q}Gq\rangle}(s) &= -\frac{m_Q\langle\bar{q}g_s\sigma\cdot Gq\rangle}{48\pi^4} \int_{\alpha_{min}}^{\alpha_{max}} d\alpha \int_{\beta_{min}}^{\beta_{max}} d\beta \left\{ \frac{(1-\alpha-\beta) [3m_Q^2(\alpha+\beta) - 5\alpha\beta s]}{\alpha\beta} \right. \\
&\quad + \frac{(1-\alpha-\beta) [6m_Q^2(\alpha+\beta) - 11\alpha\beta s]}{\beta^2} - \frac{71m_Q^2(\alpha+\beta) - 105\alpha\beta s}{2\beta} \left. \right\}, \\
\rho_3^{(8)\langle\bar{q}q\rangle^2}(s) &= \frac{10(2m_Q^2 + s)\langle\bar{q}q\rangle^2}{27\pi^2} \sqrt{1 - 4m_Q^2/s}, \\
\rho_3^{(8)\langle\bar{q}q\rangle\langle\bar{q}Gq\rangle}(s) &= \frac{\langle\bar{q}q\rangle\langle\bar{q}g_s\sigma\cdot Gq\rangle}{54\pi^2} \int_0^1 d\alpha \left\{ \frac{24m_Q^4(3-\alpha)}{2(1-\alpha)\alpha^2} \delta'(s - \tilde{m}_Q^2) \right. \\
&\quad \left. + \frac{m_Q^2(24\alpha^3 - 91\alpha^2 + 54\alpha + 9)}{2\alpha(1-\alpha)^2} \delta(s - \tilde{m}_Q^2) + (13\alpha + 12)H(s - \tilde{m}_Q^2) \right\}. \tag{A6}
\end{aligned}$$

- For the current $J_{4\mu}^{(8)}$

$$\begin{aligned}
\rho_4^{(8)pert}(s) &= \frac{1}{16\pi^6} \int_{\alpha_{min}}^{\alpha_{max}} d\alpha \int_{\beta_{min}}^{\beta_{max}} d\beta \left\{ \frac{(1-\alpha-\beta)(1+\alpha+\beta) [(\alpha+\beta)m_Q^2 - \alpha\beta s]^4}{4\alpha^3\beta^3} \right. \\
&\quad \left. - \frac{m_Q^2(1-\alpha-\beta)^2(5+\alpha+\beta) [(\alpha+\beta)m_Q^2 - \alpha\beta s]^3}{9\alpha^3\beta^3} \right\}, \\
\rho_4^{(8)\langle\bar{q}q\rangle}(s) &= \frac{m_Q\langle\bar{q}q\rangle}{2\pi^4} \int_{\alpha_{min}}^{\alpha_{max}} d\alpha \int_{\beta_{min}}^{\beta_{max}} d\beta \frac{(1-\alpha-\beta) [(\alpha+\beta)m_Q^2 - \alpha\beta s] [3m_Q^2(\alpha+\beta) - 7\alpha\beta s]}{\alpha\beta^2}, \\
\rho_4^{(8)\langle GG\rangle}(s) &= -\frac{\langle g_s^2 GG\rangle}{96\pi^6} \int_{\alpha_{min}}^{\alpha_{max}} d\alpha \int_{\beta_{min}}^{\beta_{max}} d\beta \left\{ \frac{m_Q^2(1-\alpha-\beta)^2(5+\alpha+\beta) [m_Q^2(3\alpha+4\beta) - 3\alpha\beta s]}{9\alpha^3\beta} \right. \\
&\quad + \frac{7(1-\alpha-\beta)^2 [(\alpha+\beta)m_Q^2 - \alpha\beta s] [m_Q^2(13\alpha+13\beta+29) + 12\alpha\beta s]}{288\alpha^2\beta^2} \\
&\quad - \frac{m_Q^2(1-\alpha-\beta)^2 [m_Q^2(\alpha+\beta) - 2\alpha\beta s]}{\alpha^3}
\end{aligned}$$

$$\begin{aligned}
& + \frac{7 [(\alpha + \beta)m_Q^2 - \alpha\beta s] [3m_Q^2(1 + \alpha + \beta) + 4\alpha\beta s]}{48\alpha\beta} \\
& + \frac{(1 - \alpha - \beta) [(\alpha + \beta)m_Q^2 - \alpha\beta s] [m_Q^2(3 + \alpha + \beta) + 5\alpha\beta s]}{12\alpha^2\beta} \Big\}, \\
\rho_4^{(\mathbf{8})\langle\bar{q}Gq\rangle}(s) &= \frac{m_Q\langle\bar{q}g_s\sigma\cdot Gq\rangle}{48\pi^4} \int_{\alpha_{min}}^{\alpha_{max}} d\alpha \int_{\beta_{min}}^{\beta_{max}} d\beta \left\{ \frac{(1 - \alpha - \beta) [3m_Q^2(\alpha + \beta) - 5\alpha\beta s]}{\alpha\beta} \right. \\
& + \left. \frac{(1 - \alpha - \beta) [6m_Q^2(\alpha + \beta) - 11\alpha\beta s]}{\beta^2} - \frac{71m_Q^2(\alpha + \beta) - 105\alpha\beta s}{2\beta} \right\}, \\
\rho_4^{(\mathbf{8})\langle\bar{q}q\rangle^2}(s) &= \frac{10(2m_Q^2 + s)\langle\bar{q}q\rangle^2}{27\pi^2} \sqrt{1 - 4m_Q^2/s}, \\
\rho_4^{(\mathbf{8})\langle\bar{q}q\rangle\langle\bar{q}Gq\rangle}(s) &= \frac{\langle\bar{q}q\rangle\langle\bar{q}g_s\sigma\cdot Gq\rangle}{54\pi^2} \int_0^1 d\alpha \left\{ \frac{24m_Q^4(3 - \alpha)}{2(1 - \alpha)\alpha^2} \delta'(s - \tilde{m}_Q^2) \right. \\
& + \left. \frac{m_Q^2(24\alpha^3 - 91\alpha^2 + 54\alpha + 9)}{2\alpha(1 - \alpha)^2} \delta(s - \tilde{m}_Q^2) + (13\alpha + 12)H(s - \tilde{m}_Q^2) \right\}. \tag{A7}
\end{aligned}$$